Journal of Applied Polymer Science

Morphology and Microwave Absorption of Carbon Nanotube/Bismaleimide Foams

Xiao-Li Liu,[1,2] Hai-Jun Lu,[1,2] Li-Ying Xing[1,2]

[1]AVIC (Aviation Industry Corporation of China) Composite Corporation Ltd., Beijing 100030, People's Republic of China
[2]Composites and Applications Lab, Beijing Institute of Aeronautic Materials, Beijing 100095, People's Republic of China
Correspondence to: L.-Y. Xing (E-mail: lxl_nanliu@163.com)

ABSTRACT: Proper dispersion should be guaranteed when using carbon nanotubes (CNTs) as effective absorbents. Physical dispersion methods, such as mechanical mixing, ball milling, and calendering process (three-roll milling), were adopted to disperse CNTs in the bismaleimide matrix to foam. The effects of the dispersion methods on viscosity, bubble morphology, and microwave-absorbing properties at 12–18 GHz were studied. The results indicated that, three-roll milling can more efficiently separate individual CNTs from the agglomerates compared with the other two methods. This method exhibited the highest viscosity, the most irregular cell shape, and the best microwave-absorbing property. The effects of CNT concentration and foam thickness on the microwave-absorbing properties were also studied. The reflectivity decreased and the position of the reflectivity peak moved to a lower value with increase in CNT concentration and foam thickness. The foam with 30 mm thickness achieved a reflection loss below −8 dB over 3.0 GHz in the range of 13.5–16.5 GHz. The minimum value is −14.2 dB at 14.6 GHz. © 2013 Wiley Periodicals, Inc. J. Appl. Polym. Sci. **2014**, *131*, 40233.

KEYWORDS: foams; morphology; functionalization of polymers

Received 28 August 2013; accepted 26 November 2013
DOI: 10.1002/app.40233

INTRODUCTION

Microwave-absorbing materials have elicited significant interest because of their applications in commercial and military industries.[1–3] An efficient microwave-absorbing material needs to be relatively lightweight, structurally sound, and possess effective absorption in a wide band range. Structural stealthy foams and their sandwich composites are new types of composite materials that absorb electromagnetic wave and support structural loads with low weight.[4] Thus, these materials have drawn much attention, especially in the aerospace industry. Bismaleimide (BMI)[5,6] foam is one of the most important high-performance foams because of its excellent heat resistance and high specific strength; however, BMI radar-absorbing foam has not been studied to date.

The manufacture[7,8] of microwave-absorbing materials involves the use of compounds capable of generating dielectric and/or magnetic losses that enable them to absorb incident radiation in synchronized frequencies and dissipate it as heat. Carbon nanotubes (CNTs) are lightweight materials, that have strong microwave absorption properties in the GHz frequency range.[9–12] Nanometer-scale diameter CNTs can avoid the limitation of large-sized conventional conductivity fillers, and their extremely large aspect ratio allows low loading of fillers to provide the desired electrical conductivity without sacrificing other inherent properties of the polymer. Therefore, CNTs are ideal fillers for preparing microwave-absorbing composites. Fan et al.[13] prepared CNT/polymer [polyethylene terephthalate (PET), polypropylene (PP), polyethylene (PE), and varnish] composites, and studied their microwave-absorbing properties. They observed a sharp increase in loss tangent when the CNT concentration was more than 4 wt %. The 4 wt % CNTs/PET and 8 wt % CNTs/varnish composites exhibited considerable absorbing peaks at 7.6 and 15.3 GHz, and achieved maximum absorbing values of 17.61 and 24.27 dB, respectively. Chen et al.[14] fabricated multilayered carbon nanotubes/silicon dioxide ($CNTs/SiO_2$) electromagnetic microwave-absorbing ceramic matrix composite materials by hot-pressed sintering. The gradient layer structure was designed to improve absorbing properties. The multilayered $CNTs/SiO_2$ composites were shaped by adding five kinds of mixed powders with different CNT contents of 0, 2.5, 5, 7.5, and 10 wt %. The electromagnetic were studied in the range of 8–12 GHz. The results showed that the gradient multilayered sample had better absorbing effectiveness and its absorbance was 1.5 times as high as that of the single-layered sample.

Numerous research efforts have been directed toward producing CNT/polymer composites for functional and structural applications.[15–17] However, even after a decade of research, the full potential of using CNTs as reinforcements has been severely

limited because of the difficulties associated with the dispersion of entangled CNT during processing and the poor interfacial interaction between CNTs and the polymer matrix. The nature of the dispersion problem for CNTs is rather different from those of other conventional fillers,[18] such as spherical particles and carbon fibers, because CNTs are characteristic of small diameters in nanometer scale with high aspect ratios (>1000). Consequently, their surface area is extremely large. In addition, commercialized CNTs are supplied in the form of heavily entangled bundles, resulting in inherent difficulties in dispersion.

The approaches often used to disperse CNTs are optimum physical blending and functionalization-based dispersion. The surface modification and functionalization of CNTs can enhance their interaction with the polymer matrix, thus improving their dispersion in the matrix. Some of the methods for optimum physical blending are ultrasonication, shear mixing, calendering, ball milling, stirring, and extrusion. Chen et al.[19] synthesized epoxy/CNT nanocomposites in various ways to examine the effects of dispersion methods on their tribological properties. The dispersion and mixing methods used include dual asymmetric centrifuge, sonication, and hand mixing. Wear resistance improves with increasing effort placed into dispersion: sonication has a positive effect, and sonication plus dual asymmetric centrifugation has been proven to be even better. The results showed that the wear resistance increased with improved dispersion and integrity of the CNTs.

A microwave-absorbing foam using CNT as absorbent with BMI resin as matrix was prepared in this article. The electromagnetic and microwave absorption characteristics in the range of 12–18 GHz of the CNTs and CNT/BMI foam were analyzed, respectively. The effects of physical dispersion methods (mechanical stirring, ball milling, and calender) on the bubble morphology and microwave-absorbing properties were discussed. The effects of CNT content and foam thickness on the microwave absorption properties were also investigated.

EXPERIMENTAL

Materials

The multi-wall CNTs were Flo Tube 9000 supplied by Tiannai Corporation (Beijing, China), with average length of 10 μm and average diameter of about 11 nm, and produced through catalytic vapor deposition process. Azodicarbonamide (ADC) purchased from the Letai Chemical Plant (Beijing, China) with decomposition temperature of 215°C and generated gas amount 210 mL/g was used as the blowing agent. BMI was prepared in our laboratory.

Sample Preparation

Mechanical stirring method: CNTs and BMI resin were carefully weighed and mixed in a beaker with a propeller at a certain mixing speed (300 rpm) for 20 min.

Ball milling method: BMI and CNTs were dissolved in acetone and the blend was placed into a ball mill jar with stainless steel balls. The ball-milling process was performed at 300 rpm for a certain period (up to 48 h). Afterward, the acetone was evaporated until a constant weight was achieved.

Three-roll milling method (calendering process): CNTs were manually stirred into the melt resin, and then the predispersed suspension was placed onto the rolls. The suspensions were produced using a three-cycle program with the same distances (0.5 μm) between the rolls. The speed for the apron roll was set to 300 rpm.

The obtained CNT/BMI nanocomposites through different dispersion methods were used for foaming. CNT/BMI foams were prepared through prepolymerization and foaming. The suspension was heated to 140°C and maintained at this temperature for 30 min. Afterward, 5 wt % ADC was added to the melted prepolymer with constant stirring. The mixture was placed into a preheated mold (180°C) for foaming and curing. Details about the foaming technique can be also found in earlier publications.[5,6]

Viscosity

The changes in viscosity were determined at constant temperature of 140°C using an AR 2000 (TA Instruments). The measurements were performed at constant angular frequency of 1.0 rad/s, with 1% strain.

Scanning Electron Microscopy Observations

The fractured cross-sections of the BMI/CNT nanocomposites with different dispersion methods were gold sputtered and observed under a scanning electron microscope (SEM; Camscan 3100, Britain).

The fractured cross-sections of the foamed samples coated with gold were observed under SEM. The average diameters of the bubbles were calculated using image-processing software (Image-Pro Plus). Cell diameter (D) was computed as the average of the diameters of all the cells on the SEM micrograph, and more than 100 cells were measured. The formula is as follows,

$$D = \frac{\sum d_i n_i}{n_i}$$

where n_i is the number of cells with a perimeter-equivalent diameter of d_i.

Microwave-Absorbing Properties

Electromagnetic Parameters of CNTs. To explore the intrinsic reasons for the microwave absorption of CNTs, 10 wt % CNTs were mixed with paraffin and prepared as hollow pipes with the size of 3 (inner) × 7 (outer) × 2 mm (length). The complex permittivity and permeability of the CNTs were measured with the coaxial line method in 12–18 GHz.

Reflection Loss Measurement. Reflection loss was measured using an HP 8722ES vector network analyzer operating at 12–18 GHz band. The area of the sample was 180 × 180 mm and the thickness was 10, 20, and 30 mm, respectively.

RESULTS AND DISCUSSION

Dispersion of CNTs in the BMI Matrix

In terms of nanotube dispersion, the two main approaches followed are categorized as mechanical/physical and chemical. The techniques affecting the chemical structure of CNTs under chemical methods (e.g., functionalization, covalent bonding,

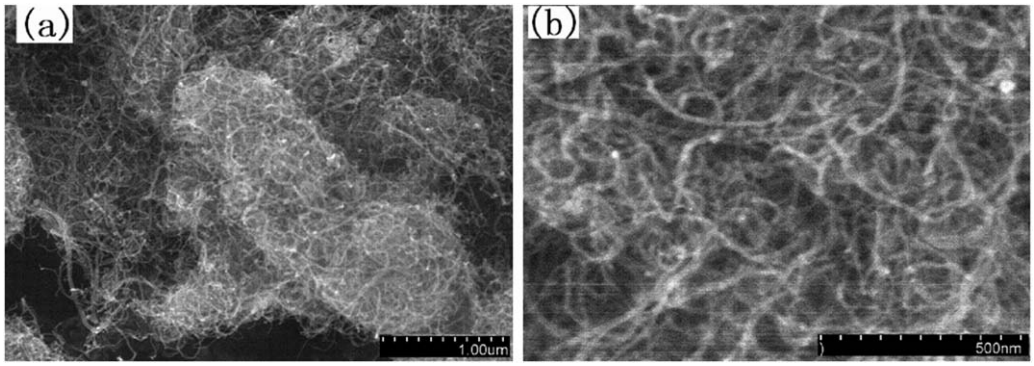

Figure 1. SEM images of the carbon nanotubes.

and incorporation of other atoms in the carbon lattice) are not the focus of this article. Mechanical dispersion methods such as mechanical stirring, ball milling, and calender process, which have little effect on the structure of CNTs, were selected in this article.

Figure 1 shows the configuration of CNTs, in which the CNTs exhibited the characteristic of nanoscale-sized diameter with high aspect ratio (10^3), and thus, extremely large surface area. CNTs are in the form of heavily entangled bundles mainly because of their tendency to agglomerate and entangle due to the strong van der Waal bonds, which become predominant as the CNT length increases. Subsequently, the lack of functional sites on the CNT surface also complicates the dispersion issue. To disperse the entangled CNTs and improve the interfacial interaction between CNTs and BMI matrix, three different physical dispersion routes to disperse CNTs homogeneously with the matrix were investigated.

Figure 2 shows the SEM of the fractured cross-section of CNT/BMI nanocomposites prepared by different mixing methods, where the right column was the magnified observation of the left one. For the mechanical stirring method, large CNTs agglomerates (about 5 to 10 μm) were observed in the composites, as shown in Figure 2(a). Although shear force and mixing energy are produced during melt mixing, CNT agglomerates can still remain entangled because of the strong intermolecular van der Waals interactions among the nanotubes. For the ball milling method, the CNT agglomerates are smaller (about 2 to 3 μm), indicating the presence of relatively thin CNT bundles and partially disentangled CNTs inside the BMI matrix, as shown in Figure 2(b). During the milling, high pressure is generated locally because of the collision between the tiny, rigid balls in a concealed container, which partially disentangled the CNTs from the agglomerates. As shown in Figure 2(c), CNTs are uniformly dispersed in the BMI matrix using three-roll milling. Further SEM observations show that the amount of CNTs is individually separated from the CNT agglomerates, and nearly no aggregates are observed. The calender uses high shear force created by rollers to mix, disperse, and homogenize CNTs/BMI. However, the agglomerates can be destroyed by shearing force. Big CNT agglomerates mixed with BMI can be effectively opened by high shear force created by the calender.

Viscosity of Foaming Matrix with Different Dispersion Methods

The viscosity of BMI and CNT/BMI matrix at constant temperature (140°C) is shown in Figure 3. The CNTs increase the viscosity of the BMI matrix; however, the increasing effect is affected by the dispersion methods. At the same time interval, the sample prepared by three-roll milling exhibited the highest viscosity and the one prepared by mechanical stirring represented the lowest viscosity. The SEM results showed that the calender can effectively open CNT entanglements and individually separate more CNTs from the agglomerates. More individual CNTs can effectively restrain the relaxation of BMI chains in the nanocomposites, so the viscosity is much higher than the others.

Morphology of BMI Foams with Different Dispersion Methods

The effect of dispersion methods on the CNT/BMI foam morphology and the cell size distribution can be seen in Figure 4. The cell size prepared by mechanical stirring method is about 0.38 mm and its distribution is more uniform than that of the others. The cell sizes are 0.56 and 0.69 mm for the foams prepared by ball milling and three-roll milling, and both their cell size distributions are not as uniform as the one prepared by mechanical stirring. This finding demonstrates that the morphology of the cell structure prepared by mechanical stirring is more uniform and nearly not affected by the presence of the CNTs. When the composites dispersed by mechanical stirring are foaming, blowing agent ADC generates gas, and the gas swells out isotropically because of the homogenous matrix, which is basically the same as the foaming mechanism of plastic foams and sponges.[20] However, for the ball milling and three-roll millings methods, the gas cell expansion may be anisotropic because of the incorporation of more individual CNTs. Individual CNTs has high aspect ratio and is anisotropic. More individual carbon nanotubes can effectively restrain the relaxation of the BMI chains in the nanocomposites, so the bubble morphology extensively changed. Meanwhile, the cell sizes decreased with the addition of nanoscale particles into the polymers. This finding is attributed to the fact that more bubbles start to nucleate concurrently, resulting in less gas for bubble growth, leading to a reduction of bubble size. The cell sizes increased with increasing individual CNTs in the BMI matrix, indicating that CNTs cannot serve well as heterogeneous nucleating agents during the foaming process.

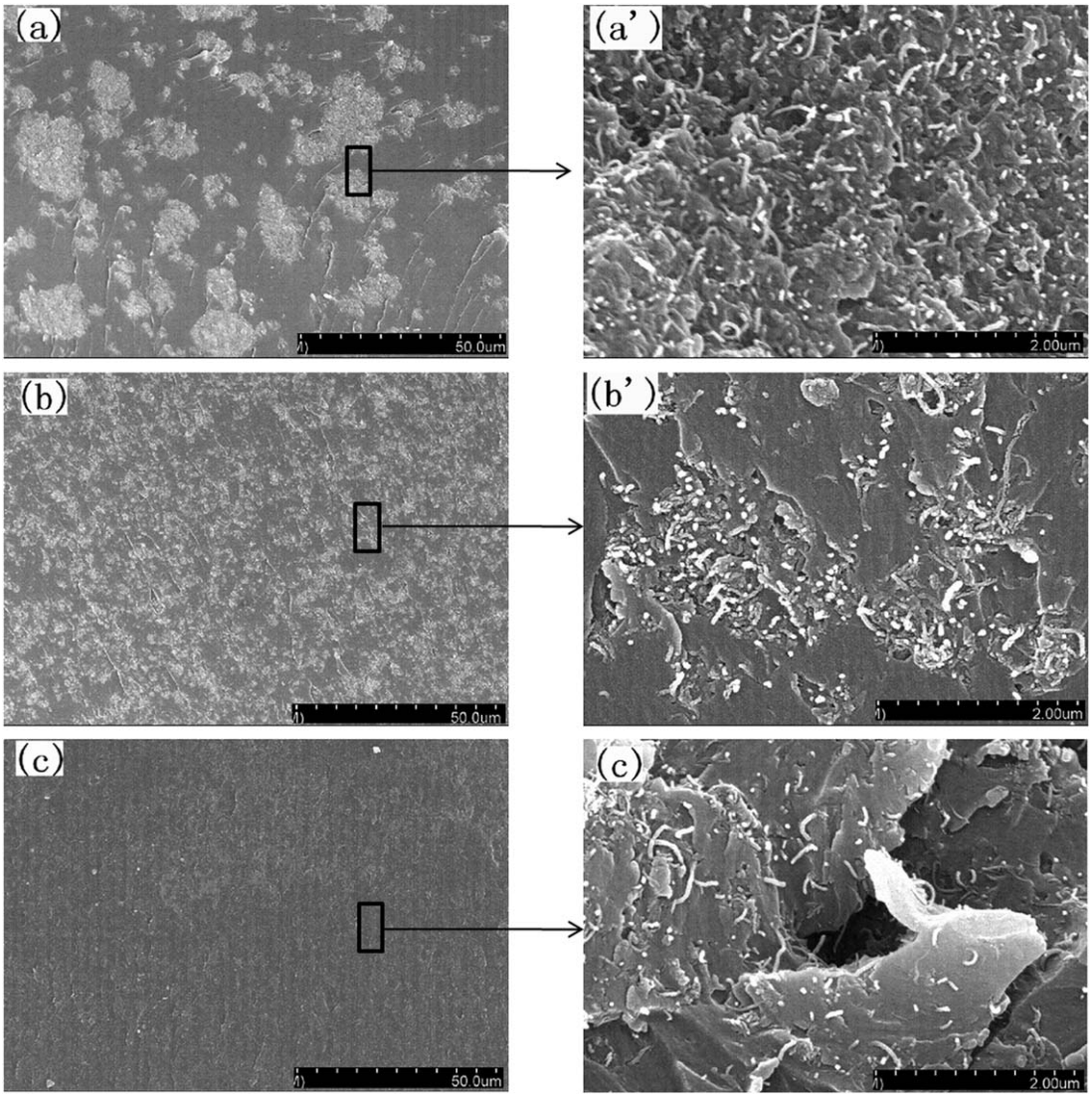

Figure 2. SEM image of the fracture surface of 1 wt % CNTs/BMI with different dispersion methods. (a) Mechanical stirring method; (b) Ball milling; (c) Three-roll milling.

Microwave-Absorbing Properties of Foams with Different Dispersion Methods

To investigate the intrinsic reasons for the microwave absorption of the CNTs/BMI foams, we measured the permittivity and permeability of CNTs using the T/R coaxial line method. The complex permittivity and permeability determine the storage capability and loss of the electromagnetic energy. Thus, they have a key role in the electromagnetic wave absorption properties of the foam. Figure 5(a) shows the real (ε') and the imaginary part (ε'') of the complex permittivity for CNTs in the frequency range of 12–18 GHz; where ε' is relative to energy storage and ε'' indicates the dielectric loss in the particle. The real and the imaginary parts of ε from 12 to 18 GHz are in the range of 23.4–18.7 and 44.9–34.1, respectively; both decrease with the increase in frequency. The real (μ') and imaginary part (μ'') of the complex permeability for the CNTs are plotted as functions of frequency (12–18 GHz) in Figure 5(b). Similar to the complex permittivity, the real part of permeability is relative

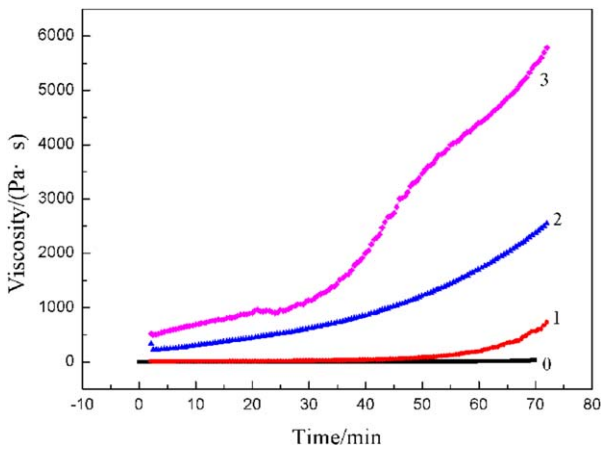

Figure 3. Viscosity of BMI and 1 wt % CNT/BMI prepared by different dispersion methods. (0 - BMI resin matrix; 1 - CNT/BMI mechanical stirring; 2 - CNT/BMI ball milling; 3 - CNT/BMI three-roll milling). [Color figure can be viewed in the online issue, which is available at wileyonlinelibrary.com.]

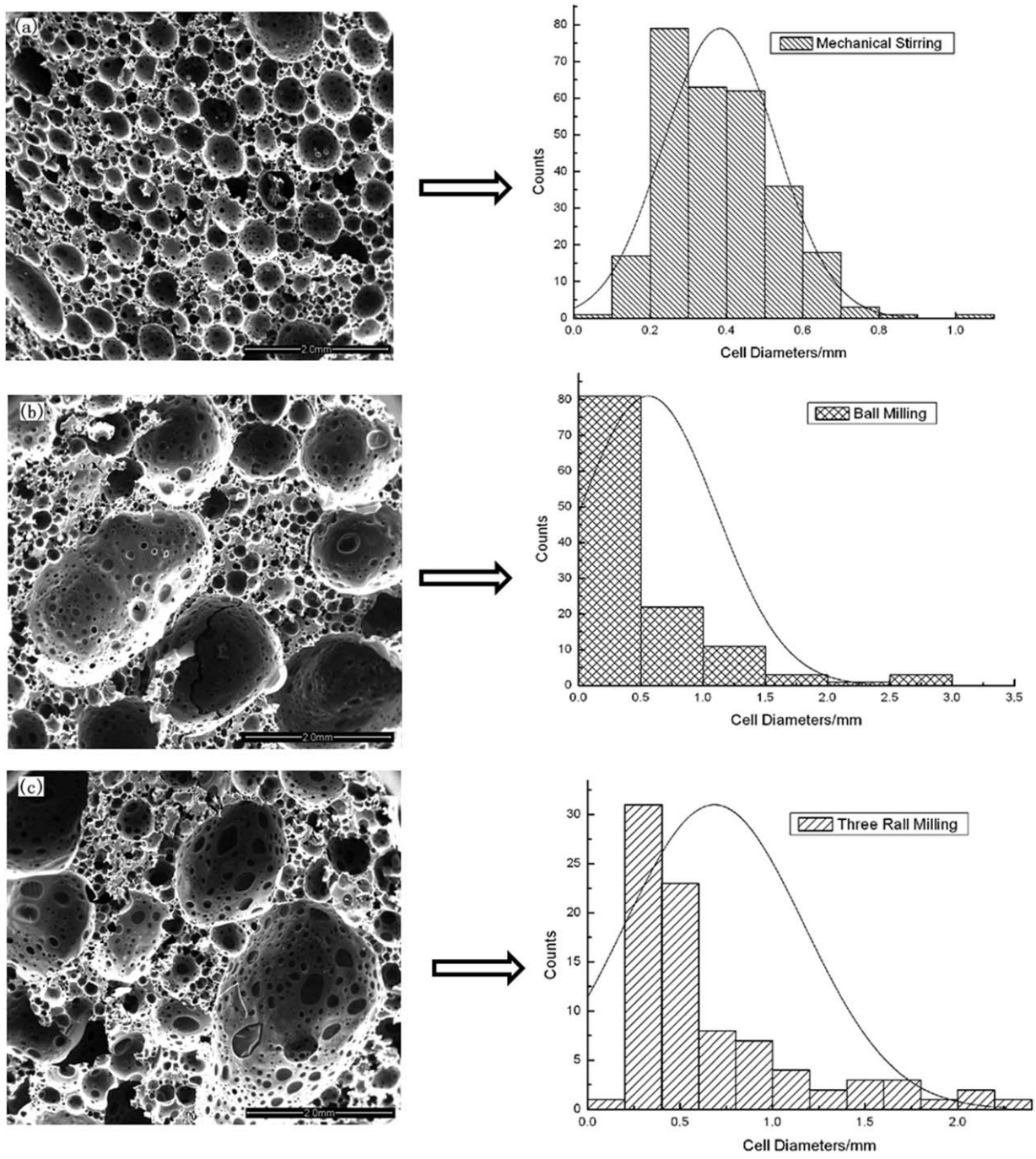

Figure 4. SEM images of CNT/BMI foams and cell size distributions prepared by different dispersion methods (1 wt % CNTs; density, 160 kg/m^3). (a) Mechanical stirring; (b) Ball milling; (c) Three-roll milling.

to energy storage and the imaginary part indicates the energy loss in the particle. The μ' and μ'' are 1.0 and 0.1 at 12 GHz, and are almost unchangeable from 12 to 18 GHz, suggesting that the microwave absorption enhancement of the foam results mainly from dielectric loss rather than magnetic loss.[21]

Figure 6 shows the frequency dependence of the reflection loss of the CNT/BMI foams prepared through different dispersion methods. The dispersion methods have an obvious effect on microwave-absorbing properties. The foam prepared by three-roll milling achieves the lowest reflection in the range of 12–18 GHz compared with the other two methods; the absorption peak is −4 dB at 18 GHz. This finding is related to the mechanism in the microwave attenuation of CNTs. CNTs with large aspect ratio (10^3) are used as dipoles to absorb the microwave in the foams. In the microwave-absorbing material containing electromagnetic loss substance and dipoles, the dipoles act as electron couplers and can generate inductive current in the electromagnetic field. The inductive current then causes

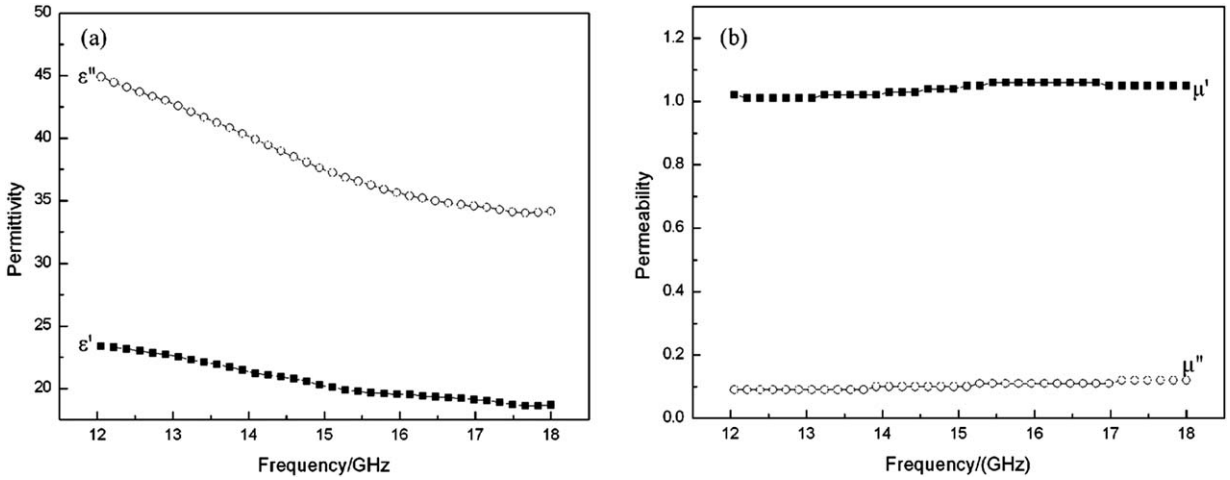

Figure 5. Electromagnetic parameters of CNTs (method described in the section electromagnetic parameters of CNTs).

current loss and energy dissipation. The interactions of the microwave electric field with charge dipoles cause crystal lattice libration, resulting in microwave energy losses through heating. For the calender process, the foam incorporates more individual CNTs, that is, more dipoles to dissipate electromagnetic wave and better microwave absorbing properties.

CNT Concentration on Microwave-Absorbing Properties

To obtain better microwave absorbing properties, the three-roll milling method was used to disperse CNTs in the BMI matrix. The effect of CNT concentration on the microwave-absorbing properties is shown in Figure 7. Viscosity is a key parameter that controls the stabilization of the expanding structure in foams. The addition of CNTs into the BMI matrix rapidly increases the viscosity, reaching a tar-like[21] consistency of about 1.5 wt %. The system can no longer be foamed properly at CNT loading fractions above 1 wt % because of this viscosity increase. Clearly, the reflectivity decreases and the position of the reflectivity peak moves to a lower value as the CNT concentration increases in the 12–18 GHz range because ε increases with increasing CNT concentration. In addition, the more CNT particles in the matrix per unit volume, the more surface areas are provided to attenuate the electromagnetic wave by multi-scatter and reflection. CNTs with higher aspect ratio result in better microwave-absorbing properties than spherical or elliptical fillers at the same filler concentrations in forming conducting networks in polymer matrices.[10] Meanwhile, due to viscosity increase, manipulating absorbing properties by changing the CNT concentrations is difficult.

Thickness of Foams on Microwave-Absorbing Properties

The effect of thickness on the absorption curve is shown in Figure 8, wherein as foam thickness increases, the reflection decreases and the reflectivity peak moves to lower frequency. The foam with 30 mm thickness achieves a reflection loss below −8 dB over 3.0 GHz in the range of 13.5–16.5 GHz. The minimum value is −14.2 dB at 14.6 GHz. The thickness increase brings more reflection loss and scatters microwave in the foam. Increasing foam thickness can improve the microwave

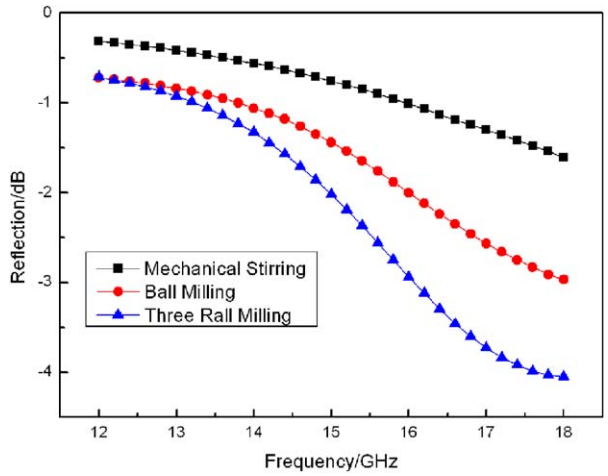

Figure 6. Reflection curves of CNT/BMI foam prepared by different dispersion methods. (1 wt % CNTs; thickness, 10 mm; foam density, 160 kg/m^3). [Color figure can be viewed in the online issue, which is available at wileyonlinelibrary.com.]

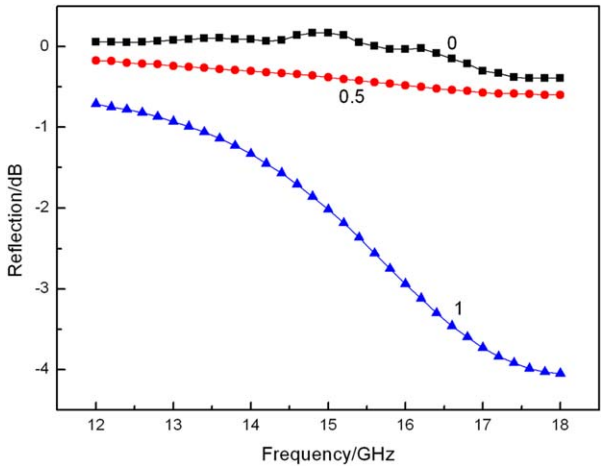

Figure 7. Absorption curves of the samples with different CNT concentrations (thickness, 10 mm). [Color figure can be viewed in the online issue, which is available at wileyonlinelibrary.com.]

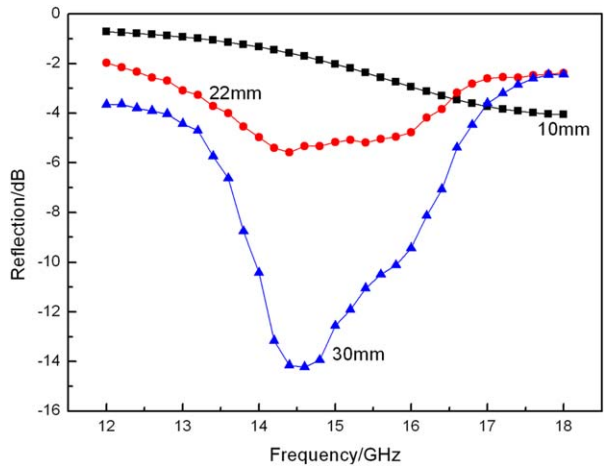

Figure 8. Absorption curves of CNT/BMI foams with different thicknesses (CNT concentration, 1 wt %). [Color figure can be viewed in the online issue, which is available at wileyonlinelibrary.com.]

absorption properties in the lower frequency range. The phenomenon can be explained by the following equation:[22]

$$f_m = \frac{C}{2\pi\varepsilon'' d}$$

where f_m, C, and d are the matching frequency (the frequency of absorption peak), the velocity of light, and the sample thickness, respectively, and ε'' is the imaginary part of complex permittivity representing the dielectric loss in CNTs. This equation indicates that the matching frequency f_m shifts toward lower frequency with increasing sample thickness. Therefore, the microwave absorption properties of the samples can be modulated by thickness.

CONCLUSIONS

The morphology and the microwave absorbing properties in the range of 12–18 GHz of CNT/BMI foams were investigated. Compared with mechanical stirring and ball milling, the three-roll milling method can more efficiently separate individual CNTs from the agglomerates. This process leads to the highest viscosity, the most irregular cell shape, and the best microwave-absorbing properties.

The microwave-absorbing properties are affected by CNT concentration and foam thickness. The reflectivity decreases and the position of the reflectivity peak moves to a lower value as the CNT concentration and thickness increase. The foam (1 wt % CNT concentration) with 30 mm thickness achieved a reflection loss below −8 dB over 3.0 GHz in the range of 13.5–16.5 GHz, with a minimum value −14.6 dB at 14.2 GHz.

REFERENCES

1. Liu, Z. F.; Bai, G.; Huang, Y.; Li, F. F.; Ma, Y. F. *J. Phys. Chem.* **2007**, *111*, 13696.
2. Tong, G. X.; Wu, W. H.; Hua, Q.; Miao, Y. Q.; Guan, J. G.; Qian, H. S. *J. Alloy. Compd.* **2011**, *509*, 451.
3. Tsay, C. Y.; Yang, R. B.; Hung, D. S.; Hung, Y. H.; Yao, Y. D.; Lin, C. K. *J. Appl. Phys.* **2010**, *107*, 502.
4. Zeng, C. C.; Hossieny, N.; Zhang, C.; Wang, B. *Polymer* **2010**, *51*, 655.
5. Liu, X. L.; Lu, H. J.; Xing, L. Y. *Int. Polym. Proc.* **2012**, *5*, 617.
6. Liu, X. L.; Lu, H. J.; Xing, L. Y. *J. Mater. Eng.* **2012**, *8*, 83.
7. Yan, D. X.; Dai, K.; Xiang, Z. D.; Li, Z. M.; Ji, X.; Zhang, W. Q. *J. Appl. Polym. Sci.* **2011**, *120*, 3014.
8. Chen, L. M.; Schadler, L. S.; Ozisik, R. *Polymer* **2011**, *52*, 2899.
9. Zhang, L.; Zhu, H.; Song, Y.; Zhang, Y. M.; Huang, Y. *Mater. Sci. Eng. B* **2008**, *153*, 78.
10. Zhao, D. L.; Li, X.; Shen, Z. M. *Compos. Sci. Technol.* **2008**, *68*, 2902.
11. Zhao, D. L.; Li, X.; Shen, Z. M. *Mater. Sci. Eng. B* **2008**, *150*, 105.
12. Rosa, I. M.; Dinescu, A.; Sarasini, F.; Sarto, M. S.; Tamburrano, A. *Compos. Sci. Technol.* **2010**, *70*, 102.
13. Fan, Z. J.; Luo, G. H.; Zhang, Z. F.; Zhou, L.; Wei, F. *Mater. Sci. Eng. B* **2006**, *132*, 85.
14. Chen, M. X.; Zhu, Y.; Pan, Y. B.; Kou, H. M.; Xu, H.; Guo, J. K. *Mater. Design* **2011**, *32*, 3013.
15. Ma, P. H.; Siddiqui, N. A.; Marom, G.; Kim, J. K. *Compos. Part A-Appl. Sci.* **2010**, *41*, 1345.
16. Kasaliwal, G. R.; Pegel, S.; Goldel, A.; Potschke, P.; Heinrich, G. *Polymer* **2012**, *51*, 2708.
17. Gkikas, G.; Barkoula, N. M.; Paipetis, A. S. *Compos. Part B-Eng.* **2012**, *43*, 2697.
18. Zhou, Z.; Wang, S. F.; Zhang, Y.; Zhang, Y. X. *J. Appl. Polym. Sci.* **2006**, *102*, 4823.
19. Chen, H. Y.; Jacobs, O.; Wu, W.; Rudiger, G.; Schadel, B. *Polym. Test.* **2007**, *26*, 351.
20. Lin, G.; Zhang, X. J.; Liu, L.; Zhang, J. C.; Chen, Q. M.; Zhang, L. Q. *Eur. Polym. J.* **2004**, *40*, 1733.
21. Liu, L. D.; Duan, Y. P.; Ma, L. X.; Liu, S. H.; Yu, Z. *Appl. Surf. Sci.* **2010**, *257*, 842.
22. Verdejo, R.; Stampfli, R.; Alvarez-Lainez, M.; Mourad, S.;Perez, M. A.; Bruhwiler, P. A.; Shaffer, M. *Compos. Sci. Technol.* **2009**, *69*, 1564.